ACS OMEGA

http://pubs.acs.org/journal/acsodf

Article

Ternary and Quaternary Nanocrystalline Cu-Based Sulfides as Perspective Antibacterial Materials Mechanochemically Synthesized in a Scalable Fashion

Matej Baláž,* L'udmila Tkáčiková, Martin Stahorský, Mariano Casas-Luna, Erika Dutková, Ladislav Čelko, Mária Kováčová, Marcela Achimovičová, and Peter Baláž

Cite This: *ACS Omega* 2022, 7, 27164−27171

Read Online

ACCESS | Metrics & More | Article Recommendations | Supporting Information

ABSTRACT: Twelve Cu-based ternary (Cu−Me_1−S, Me_1 = Fe, Sn, or Sb) and quaternary (Cu−Me_2−Sn−S, Me_2 = Fe, Zn, or V) nanocrystalline sulfides are shown as perspective antibacterial materials here. They were prepared from elemental precursors by a one-step solvent-free mechanochemical synthesis in a 100 g batch using scalable eccentric vibratory ball milling. Most of the products have shown strong antibacterial activity against *Escherichia coli* and *Staphylococcus aureus* bacteria. For instance, stannite Cu_2FeSnS_4 and mohite Cu_2SnS_3 were the most active against *E. coli*, whereas kesterite Cu_2ZnSnS_4 and rhodostannite $Cu_2FeSn_3S_8$ exhibited the highest antibacterial activity against *S. aureus*. In general, stannite has shown the best antibacterial properties out of all the studied samples. Five out of twelve products have been prepared using mechanochemical synthesis for the first time in a scalable fashion here. The presented synthetic approach is a promising alternative to traditional syntheses of nanomaterials suitable for biological applications and shows ternary and quaternary sulfides as potential candidates for the next-generation antibacterial agents.

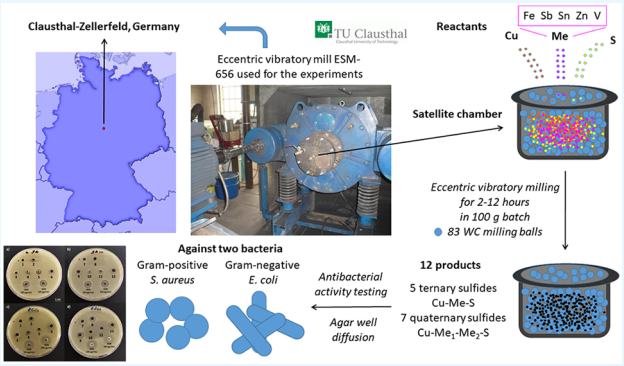

1. INTRODUCTION

Contemporary human society is confronted with several critical concerns, and infection diseases are among the most important ones.[1] Antibiotics worked very well against bacteria in the past. However, nowadays, antimicrobial resistance has been reaching a critical level.[2] Insight into new antibacterially active materials, not yet known to the microbes, is therefore a reasonable approach. Finding a chemically stable, non-toxic, and low-cost antibacterial material is of utmost importance. Metal sulphides mimicking safe natural minerals seem to be rising stars in this area.[1,3] More binary metal sulphides perfectly serve this role. The antibacterial potential of Ag_2S,[4−8] CdS,[9−17] CuS[18−27] MoS_2,[28−38] and ZnS[39−44] has been studied many times. There are few publications on the antimicrobial action of more exotic binary sulfides like SnS_2,[45] CoS_2,[46] NiS,[47] and In_2S_3.[48] Binary sulfides are most often complemented by another compounds like oxides to get the composite with good antibacterial activity. The works on the antibacterial activity of ternary and quaternary sulfides are even more scarce, namely just the antibacterial potential of Cu_2SnS_3,[49] Cu_2ZnSnS_4,[50,51] and $Cu_{12}Sb_4S_{13}$[52] has been discovered so far.

There are many synthetic pathways for sulfide nanoscale production,[3,53,54] among which a scalable, solvent-free one-step methodology called mechanochemical synthesis has found an inevitable place.[55,56] One of the scalable alternatives to the lab-scale mechanochemical synthesis is eccentric vibratory milling[57] and it has been sufficiently applied to prepare both sulfides[58−65] and selenides.[66]

This article provides a comprehensive viewpoint on the antibacterial potential of twelve Cu-based ternary and quaternary sulfides mechanochemically synthesized in a scalable fashion. For the most of the products, the antibacterial activity has not been reported yet. Moreover, five of them have not even been prepared mechanochemically so far. As the eccentric vibratory mill used for the experiments in this study was located at Technical University of Clausthal, Germany, a birthplace of famous microbiologist Robert Koch,[67] the samples in this study are labeled as KOCH*x* (*x* being a sample number), as a tribute to him.

Received: March 18, 2022
Accepted: June 2, 2022
Published: July 26, 2022

Table 1. Weights of the Precursors and Milling Time for the Mechanochemical Syntheses of Ternary and Quaternary Cu-Based Sulfides Synthesized in this Study[a]

			weight (g)					milling time (min)
sample	desired phase	phase name	Cu	Fe	Sb	Sn	S	
KOCH 1	$CuFeS_2$	chalcopyrite	34.6	30.4			35.0	720
KOCH 2[58]	$Cu_6Fe_2SnS_8$	mawsonite	53.9	12.9		13.7	29.5	240
KOCH 3	$Cu_6FeSn_2S_8$	chatkalite	41	6		25.5	27.5	120
KOCH 4	$Cu_8Fe_3Sn_2S_{12}$	stannoidite	39.2	12.9		18.3	29.6	120
KOCH 5[59]	$Cu_2FeSn_3S_8$	rhodostannite	16	7		32.2	44.8	600
KOCH 6[60]	Cu_2ZnSnS_4	kesterite	28.9	14.9		27.0	29.2	360
KOCH 7[61]	$Cu_{12}Sb_4S_{13}$	tetrahedrite	45.8		29.2		25.0	240
KOCH 8[62]	$Cu_{13}VSn_3S_{16}$	colusite	47.3			20.4	29.4	720
KOCH 9[63]	Cu_2SnS_3	mohite	37.2			34.7	28.1	180
KOCH 10[64]	Cu_3SbS_4	famatinite	43.3		27.6		29.1	240
KOCH 11	Cu_3SbS_3	skinnerite	46.7		29.8		23.5	120
KOCH 12	Cu_2FeSnS_4	stannite	29.6	13.0		27.6	29.8	120

[a]For colusite (KOCH8), also 2.9 g of vanadium was used for the synthesis.

2. MATERIALS AND METHODS

2.1. Materials. For mechanochemical synthesis of chalcopyrite $CuFeS_2$, chatkalite $Cu_6FeSn_2S_8$, stannoidite $Cu_8Fe_3Sn_2S_{12}$, skinnerite Cu_3SbS_3, and stannite Cu_2FeSnS_4, the following precursors were used: copper (Merck, Germany, 99,7% purity), antimony (Merck, Germany, 99.8% purity), tin (Nihon Seiko, Japan, 99% purity), iron (WINLAB, Germany, 99% purity), and sulfur (CG-Chemikalien, Germany, 99% purity).

2.2. Mechanochemical Synthesis. The details on the mechanochemical syntheses of the majority of the studied compounds can be found in the following publications: mawsonite $Cu_6Fe_2SnS_8$,[58] rhodostannite $Cu_2FeSn_3S_8$,[59] kesterite Cu_2ZnSnS_4,[60,65] tetrahedrite $Cu_{12}Sb_4S_{13}$,[61] colusite $Cu_{13}VSn_3S_{16}$,[62] mohite Cu_2SnS_3,[63] and famatinite Cu_3SbS_4.[64] The weights of precursors for all the compounds (including those newly prepared) and the corresponding milling time are provided in Table 1.

The rest of the milling conditions was similar for all the samples. The mechanochemical syntheses were carried out in an industrial eccentric vibratory ball mill ESM 656-0.5ks (Siebtechnik, Germany) working under the following conditions: A 5 L steel satellite milling chamber attached to the main corpus of the mill, 83 tungsten carbide balls with a diameter of 35 mm and a total mass of 30 kg, 80% ball filling in the milling chamber, amplitude of inhomogeneous vibrations 20 mm, rotational speed of the eccenter 960 min^{-1}, and an argon atmosphere. The total feed of reaction precursors was 100 g per batch. The milling was performed for different times which are mentioned in the appropriate sections.

2.3. Characterization. *2.3.1. X-ray Diffraction.* The phase composition of all mechanochemically prepared products was analyzed by X-ray diffraction (XRD, Rigaku SmartLab 3 kW) in a Bragg−Brentano geometry in a 2θ-angle range of 10−90° using Cu Kα radiation with 30 kV and 40 mA and a scan speed of 4° min^{-1}. The phase identification in the acquired XRD patterns was performed using the HighScore Plus software (PANalytical B.V., The Netherlands, version 3.0e) in the 2θ-angle range of 15−65°.

2.3.2. ζ-Potential Measurements. ζ-potential was measured in the diluted water solution of sodium chloride (10 mM) using Zetasizer Nano ZS (Malvern, Malvern, U.K.) setup, the electrophoretic mobility of the particles being converted to zeta potential using the Smoluchowski equation built in the Malvern Zetasizer software. The measurements were performed in triplicate with at least 12 sub-runs for each sample.

2.4. Antibacterial Activity. The antibacterial properties of the samples were evaluated by the agar well diffusion method by a slight modification in the process reported in.[68] The tested bacteria (*Staphylococcus aureus* CCM 4223 and *Escherichia coli* CCM 3988) were obtained from the Czech collection of microorganisms (CCM, Brno, Czech Republic). The procedure used was as follows:

- Bacteria were cultured overnight, aerobically at 37 °C in Luria−Bertani (LB) medium (Sigma-Aldrich, Saint-Louis, MO) with agitation. After this, bacteria were mixed with 50% glycerol (Mikrochem, Pezinok, Slovakia) and frozen glycerol stock cultures were maintained at −20 °C. Before the experimental use, cultures were transferred to LB medium and incubated for 24 h, and used as the source of inoculum for each experiment.
- Plate count agar (HIMEDIA, Mumbai, India) medium was cooled to 42 °C after autoclaving, inoculated overnight with liquid bacterial culture to a cell density of 5×10^5 colony-forming units per mililiter (cfu/mL).
- 20 mL of this inoculated agar was pipetted into a 90 mm diameter Petri dish.
- Once the agar was solidified, five mm diameter wells were punched in the agar and filled with 50 μL of samples prepared in the form of suspensions (prepared by dispersing 20 mg of KOCH*x* samples in 1 mL of distilled water). Gentamicin sulfate (Biosera, Nuaille, France) with the concentration of 30 mM was used as a positive control.
- The plates were incubated for 24 h at 37 °C.
- Afterward, the plates were photographed and the inhibition zones were measured by the ImageJ 1.53e software (National Institutes of Health, Bethesda, MD). The values used for the calculation are mean values obtained from 3 replicate tests.

The antibacterial activity was calculated by applying the formula reported in:[68] %Relative inhibition zone diameter (RIZD = [(IZD sample − IZD negative control)/IZD gentamicin] × 100, where RIZD is the relative inhibition zone diameter (%) and IZD is the inhibition zone diameter

https://doi.org/10.1021/acsomega.2c01657
ACS Omega 2022, 7, 27164−27171

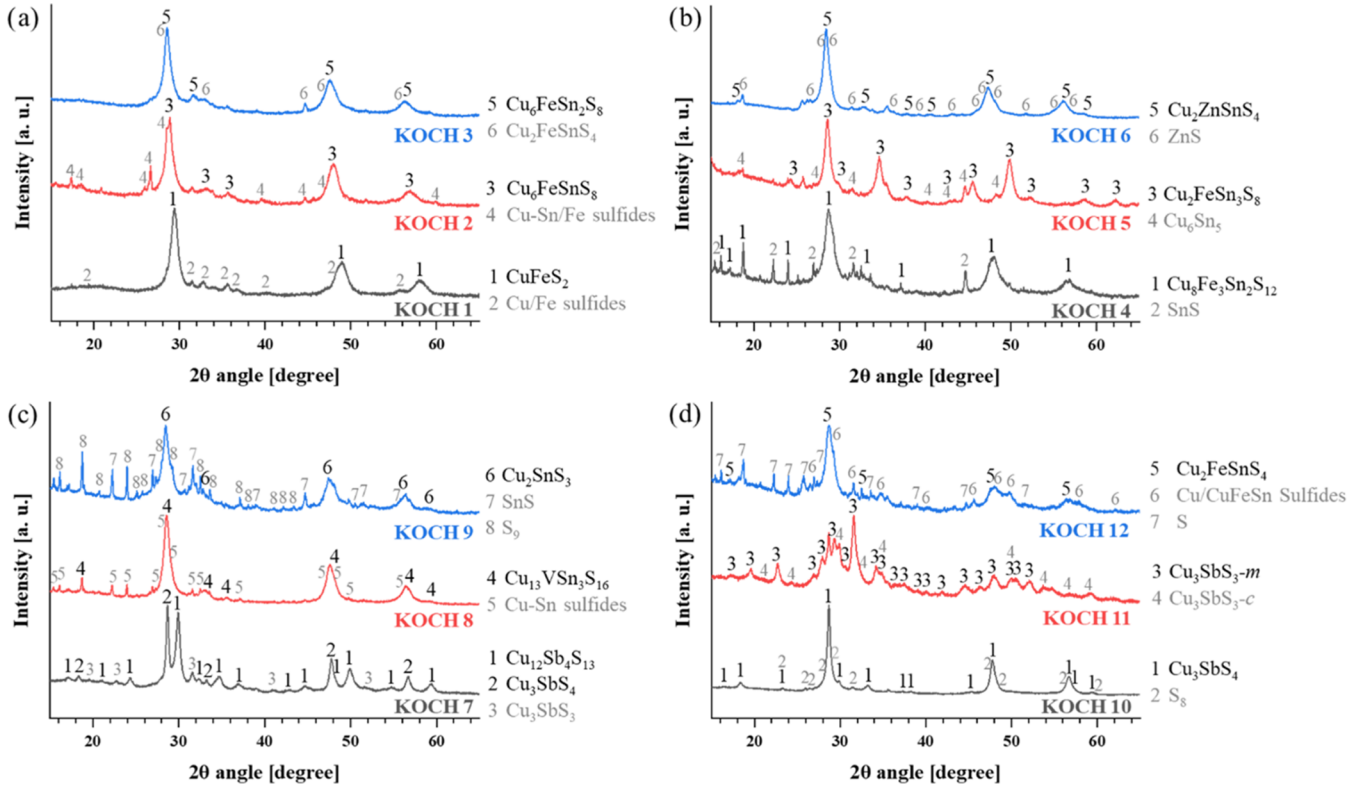

Figure 1. XRD patterns of all powders under study containing mostly ternary and quaternary sulfides: (a) KOCH 1-3, (b) KOCH 4-6, (c) KOCH 7−9, (d) KOCH 10−12. High-intensity diffraction peaks are marked in black for the main present phase, additional secondary phases are marked in grey for each system.

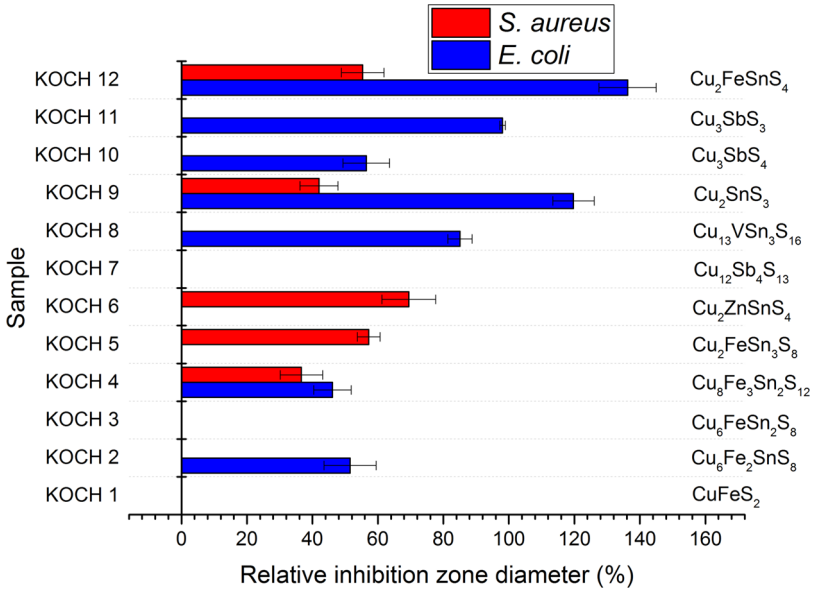

Figure 2. Relative inhibition zone diameter (RIZD) for all twelve studied samples for both *S. aureus* and *E. coli*. The positive control was antibiotic gentamicin with a concentration of 30 μg/mL and its RIZD was taken as 100%.

(mm). As a negative control, the inhibition zones of distilled water equal to 0 were taken. The inhibition zone diameter (IZD) was obtained by measuring the diameter of the transparent zone and subtracting the size of the wells (5 mm).

3. RESULTS AND DISCUSSION

3.1. X-ray Diffraction. The formation of nanoparticles by mechanochemistry is well-known.[55,69] In general, two phenomena are observed during high-energy milling, mechanical activation and mechanochemical reaction.[70,71] While the first one can be considered a top-down approach (by diminishing the crystallite size down to the nanoscale), the second one might also be considered as a bottom-up strategy, as the size of the produced nanoparticles can be increased with prolonged milling. The particle size of the precursors is being reduced down to the nanoscale and simultaneously, the

https://doi.org/10.1021/acsomega.2c01657
ACS Omega 2022, 7, 27164−27171

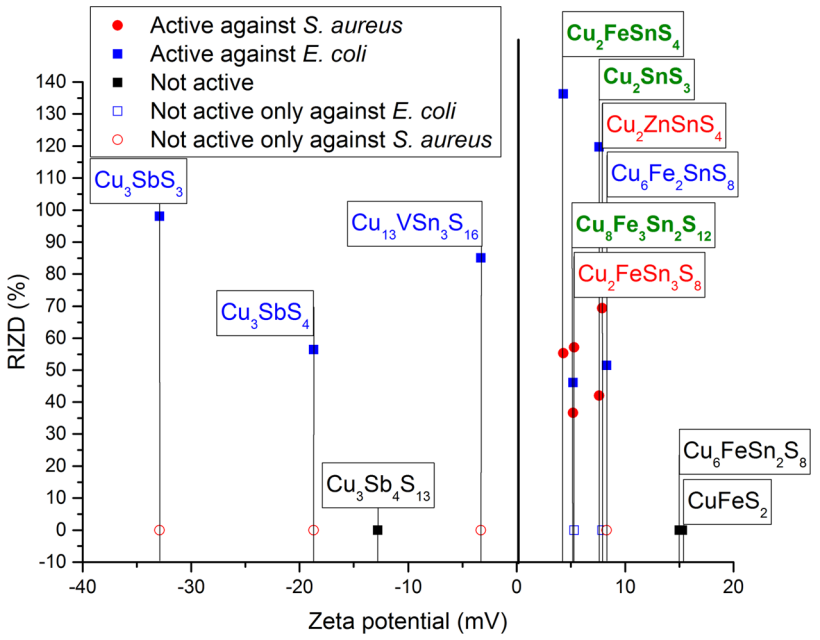

Figure 3. Dependence of antibacterial activity expressed as RIZD on ζ-potential. The formulas of the main phases in the samples are in different color: green- active against both bacteria, red—active only against *S. aureus*, blue—active only against *E. coli*, black—not active against either bacteria.

reaction between them occurs on the grain boundaries. The produced nanoparticles are most often present in the form of microcrystalline agglomerates; however, the X-ray diffraction usually reveals nanoscale dimensions of the individual crystallites.

The XRD patterns of all the samples synthesized in the present study and their principal identified phases are provided in Figure 1.

The mechanochemical syntheses of ternary and quaternary Cu sulfides represent an excellent scalable method to obtain a predetermined Cu−sulfide phase.[63,65] In general, all samples were composed of the desired ternary or quaternary copper sulfide as a major phase. However, secondary phases were also present either as a result of an incomplete reaction between the initial reactants or because of the fact that they represent intermediate phases formed on the reaction pathway to the desired compound. A significant peak broadening clearly shows the nanocrystalline character of the products, and this has been also confirmed by calculations from XRD data and transmission electron microscopy (TEM) analysis for seven products that have been synthesized before.[58−65]

It can be deduced that the secondary phases are present in small amounts by comparing the peak intensities of the identified phases in each processed system. Only in the synthesis of tetrahedrite ($Cu_{12}Sb_4S_{13}$, KOCH7 sample), similar peak intensity of famatinite (Cu_3SbS_4) was registered. The presence of secondary phases is something that must be followed for scalable intentions in potential industrial applications, especially if the presence of a specific secondary phase compromises the antibacterial activity of the final product. This can be exemplified in the KOCH7 system, where neither of the two ternary Cu-based sulfides did contribute to the antibacterial response, as will be shown later.

An overview of the identified phases in each processed sample, together with their crystallographic information references or synthesis methodologies is provided in the supplementary material (Table S1).

3.2. Antibacterial Activity. *3.2.1. Relative Inhibition Zone Diameter (RIZD) determination using the agar well diffusion method.* Twelve Cu-based sulfides were subjected to antibacterial tests using the agar well diffusion method. The relative inhibition zone diameters (RIZDs) received for both bacterial strains are summarized in Figure 2 and representative images from the experiments can be seen in the supporting file (Figure S1).

It can be seen that only three samples did not exhibit any antibacterial activity, namely chalcopyrite $CuFeS_2$, chatkalite $Cu_6FeSn_2S_8$, and tetrahedrite $Cu_{12}Sb_4S_{13}$. Out of these three compounds, only the antibacterial potential of tetrahedrite has been revealed so far.[52] In the mentioned study, the *E. coli* bacteria could be almost completely destroyed by the $Cu_{12}Sb_4S_{13}$ film in 10 min. The fact that tetrahedrite was not active in our case might be connected with the difference in the methodology used to prepare the material, which results in dissimilar properties (e.g., in nonidentical particle size).

For all other nine samples, at least some activity could be observed. In general, the activity was better against gram-negative *E. coli* (7 out of 12 investigated samples were active and RIZD values were slightly larger for the other bacteria). In the case of gram-positive *S. aureus*, the activity was registered in 5 out of 12 samples. Interestingly, different compounds were active against different types of bacteria, e.g., kesterite Cu_2ZnSnS_4 and rhodostannite $Cu_2FeSn_3S_8$ were active only against gram-positive *S. aureus*, whereas skinnerite Cu_3SbS_3, famatinite Cu_3SbS_4, collusite $Cu_{13}VSn_3S_{16}$, and mawsonite $Cu_6Fe_2SnS_8$ were active only against gram-negative *E. coli*. The activity against both types of bacteria was detected only scarcely (in 3 out of 12 samples), namely for stannite Cu_2FeSnS_4, mohite Cu_2SnS_3, and stannoidite $Cu_8Fe_3Sn_2S_{12}$. The highest RIZD was evidenced in the case of stannite (136.25 ± 8.6%) against *E. coli*. Against *S. aureus*, the best activity out of 12 studied samples was evidenced for kesterite Cu_2ZnSnS_4 (69.41 ± 8.21%).

https://doi.org/10.1021/acsomega.2c01657
ACS Omega 2022, 7, 27164−27171

The antibacterial potential of kesterite has already been studied earlier.[50,51] The zone of inhibition (ZOI) reported in[50] was 3 and 5 mm for *E. coli* and *S. aureus*, respectively, being in accordance with better activity of this compound against *S. aureus* observed also in our case. In the mentioned study, 1 mg of the powder was introduced into the well, which is the same as in our case (accepting the premise that the powder was homogeneously distributed in the distilled water before testing). The mechanism of antibacterial action of kesterite is most probably connected with the electrostatic interaction due to the opposite surface charges of the compound and the bacterial cell wall.[72]

The antibacterial effect of mohite Cu_2SnS_3 has been revealed by Lokhande et al. upon testing it against the same bacteria as in our case (*S. aureus* and *E. coli*). The antibacterial action was stronger against *E. coli*, similar to our study. The authors ascribed the difference to the thickness of the walls of the two bacteria, being 80 nm thick for *S. aureus* and only 10 nm thick for *E. coli*, respectively,[73] making the former one more resistant. The authors have demonstrated the damage caused to the *E. coli* and *S. aureus* cells by providing the scanning electron microscopy (SEM) images of the bacteria after being subjected to the effect of CTS nanocrystals. While *E. coli* bacterial cells' length increased as a result of the exposure to the Cu_2SnS_3 nanoparticles, the shrinkage of cellular texture and extrusion of intracellular fluids were observed in the case of *S. aureus*. Similar to kesterite, the authors also ascribe the mechanism of action to the electrostatic interaction between the oppositely charged species (positive charge of the nanoparticles and negative charge of the cell wall).[74,75]

3.2.2. Relationship between Antibacterial Action and ζ-Potential Measurements. The surface charge of the compounds, which is expressed by their ζ-potential, can play a decisive role in the antibacterial action. ζ-potential reflects the stability of the reaction systems in the form of colloidal dispersions.[76]

Therefore, ζ-potential measurements for all samples were performed. The measured values are summarized in Figure 3 and the Electronic Supporting Information (Table S2). It can be seen that the whole range of ζ-potential spanning from very negative to very positive values was evidenced in our case, the most negative being in the case of Cu_3SbS_3 (−32.9 mV) and the most positive in the case of chalcopyrite $CuFeS_2$ (15.3 mV). Similar results have been observed in the literature.[77−79] The presence of iron seems to lead to the positive ζ-potential values (KOCH 1−5, 12). This is a result of the dissolution of Fe^{2+} ions originating from iron particles and their transfer into the solution.[77] This is also the case of Zn^{2+} ions (KOCH 9).[80] On the other hand, the presence of antimony yields negative ζ-potential values (samples KOCH 7, 10 and 11), as evidenced for chalcostibite $CuSbS_2$.[78] The direct correlation between the ζ-potential values and the antibacterial action can be seen in Figure 3.

The correlation of ζ-potential values and the RIZD detected for all samples provides us with some clues. First, it seems that a very positive ζ-potential value is not beneficial, as when it was higher than 10 mV, no antibacterial action was observed. Second, there is a markable difference in the fact that ZP values are beneficial for the antibacterial action against the given bacterial species. While quite a wide range of ZP values (from almost −35 to +8 mV) are efficient against *E. coli*, there is quite a narrow window for the action against *S. aureus* (values between +4 and +10 mV). The products with the negative ZP values are not active against *S. aureus*, but are only active against *E. coli*, so there might be some correlation between the negative surface charge of the given sulfides and the properties of the gram-negative *E. coli* bacteria.

In three out of four studies reporting the antibacterial activity of the multinary sulfides published so far, the authors also determined the minimum inhibitory concentration (MIC). It is defined as the lowest concentration of a drug that will inhibit the visible growth of an organism after overnight incubation. The MIC value for CZTS nanocrystals prepared in[50] was 500 μg/mL against all tested bacteria, including *E. coli* and *S. aureus*. The antibacterial action of kesterite was tested against these bacterial cell lines (among others) also in[51] and the MIC value was in the range of 128−512 μg/mL, thus the results are in accordance. Lokhande et al.[49] observed a significant reduction in the growth of bacterial colonies (reporting this to be MIC) after the introduction of 1 and 3 mL of mohite Cu_2SnS_3 solution (solvent unspecified) for *S. aureus* and *E. coli*, respectively; thus the activity was better against *S. aureus* in this case. However, as mentioned earlier, the ZOI obtained by the agar well diffusion method in that study was larger for *E. coli* than for *S. aureus*, so the results from the two complementary methods are contradictory. In the present research, we also tried to determine the MIC value, however, as our powders are black, their dispersion in the solution with bacteria caused the solution to become opaque, which hampered the proper determination of MIC, as this is done spectrophotometrically.

CONCLUSIONS

Twelve ternary and quaternary nano-sulfides were successfully prepared by a mechanochemical one-step solvent-free synthesis in a 100 g batch using an eccentric vibratory ball mill. The synthesis is perfectly feasible just by solid-state milling of the elemental precursors, as in the majority of experiments, the desired sulfides were prepared as main phases. The agar well diffusion method has shown that at the concentration of 20 mg/mL, most of the products are efficient antibacterial agents, throwing some light on the influence of the chemical composition on the antibacterial action. In general, better activity of the studied sulfides was evidenced against gram-negative *E. coli*; however, in two cases (kesterite Cu_2ZnSnS_4 and rhodostannite Cu_3FeSnS_8), only the activity against *S. aureus* was observed. The most potent agents were found to be stannite Cu_2FeSnS_4 and mohite Cu_2SnS_3. The former one exhibited a significant antibacterial action against both types of bacteria. Only three out of twelve products (namely, chalcopyrite $CuFeS_2$, chatkalite $Cu_6FeSn_2S_8$, and tetrahedrite $Cu_{12}Sb_4S_{13}$) did not show any activity at the studied concentration. The investigation on the relationship between ζ-potential values and antibacterial activity has revealed that the products with the negative ζ-potential values were efficient only against *E. coli* bacteria, thus there might be some relationship between their negative charge and the properties of the *E. coli* cell wall. The present research has shown nanocrystalline sulfides as interesting alternatives to traditional antibacterial agents and also the robustness of the mechanochemical synthesis performed on a larger scale.

ASSOCIATED CONTENT

Supporting Information

The Supporting Information is available free of charge at https://pubs.acs.org/doi/10.1021/acsomega.2c01657.

https://doi.org/10.1021/acsomega.2c01657
ACS Omega 2022, 7, 27164−27171

Description of all identified crystallographic phases in KOCH 1−12 samples; including the crystallographic identification card numbers from Crystallography Open Database (COD); representative photographs from agar well diffusion tests showing transparent zones of the active samples; table listing the exact ζ-potential values detected for KOCH 1−12 samples (PDF)

AUTHOR INFORMATION

Corresponding Author

Matej Baláž − *Institute of Geotechnics, Slovak Academy of Sciences, 04001 Košice, Slovakia;* orcid.org/0000-0001-6563-7588; Email: balazm@saske.sk

Authors

L'udmila Tkáčiková − *Department of Microbiology and Immunology, University of Veterinary Medicine and Pharmacy, 04181 Košice, Slovakia*

Martin Stahorský − *Institute of Geotechnics, Slovak Academy of Sciences, 04001 Košice, Slovakia*

Mariano Casas-Luna − *Central European Institute of Technology, Brno University of Technology, 61200 Brno, Czech Republic*

Erika Dutková − *Institute of Geotechnics, Slovak Academy of Sciences, 04001 Košice, Slovakia;* orcid.org/0000-0002-4677-9123

Ladislav Čelko − *Central European Institute of Technology, Brno University of Technology, 61200 Brno, Czech Republic*

Mária Kováčová − *Institute of Geotechnics, Slovak Academy of Sciences, 04001 Košice, Slovakia*

Marcela Achimovičová − *Institute of Geotechnics, Slovak Academy of Sciences, 04001 Košice, Slovakia;* orcid.org/0000-0002-0533-8866

Peter Baláž − *Institute of Geotechnics, Slovak Academy of Sciences, 04001 Košice, Slovakia*

Complete contact information is available at: https://pubs.acs.org/10.1021/acsomega.2c01657

Notes

The authors declare no competing financial interest.

The raw/processed data required to reproduce these findings cannot be shared at this time due to technical or time limitations.

ACKNOWLEDGMENTS

The present study was financially supported by the Slovak Research and Development Agency under the Contract No. APVV-18-0357 and that of The Ministry of Education, Science, Research and Sport of the Slovak Republic Grant Agency (projects 2/0112/22 and 2/0103/20). This work was realized within the frame of the project, Research Centre of Advanced Materials and Technologies for Recent and Future Applications, PROMATECH, "ITMS 26220220186, supported by the Operational Program "Research and Development" financed through the European Regional Development Fund. The support of COST Action CA18112 MechSustInd (www.mechsustind.eu), supported by the COST Association (European Cooperation in Science and Technology, www.cost.eu) is also acknowledged. The authors also acknowledge very valuable pieces of advice and discussions with Dr. Adrian Augustyniak from West Pomeranian University of Technology in Szczecin (Poland).

REFERENCES

(1) Han, H. C.; Yang, J. J.; Li, X. Y.; Qi, Y.; Yang, Z. Y.; Han, Z. J.; Jiang, Y. Y.; Stenzel, M.; Li, H.; Yin, Y. X.; Du, Y.; Liu, J. R.; Wang, F. L. Shining light on transition metal sulfides: New choices as highly efficient antibacterial agents. *Nano Res.* **2021**, *14*, 2512−2534.

(2) Cohen, M. L. Changing patterns of infectious disease. *Nature* **2000**, *406*, 762−767.

(3) Coughlan, C.; Ibáñez, M.; Dobrozhan, O.; Singh, A.; Cabot, A.; Ryan, K. M. Compound Copper Chalcogenide Nanocrystals. *Chem. Rev.* **2017**, *117*, 5865−6109.

(4) Levard, C.; Hotze, E. M.; Colman, B. P.; Dale, A. L.; Truong, L.; Yang, X. Y.; Bone, A. J.; Brown, G. E.; Tanguay, R. L.; Di Giulio, R. T.; Bernhardt, E. S.; Meyer, J. N.; Wiesner, M. R.; Lowry, G. V. Sulfidation of Silver Nanoparticles: Natural Antidote to Their Toxicity. *Environ. Sci. Technol.* **2013**, *47*, 13440−13448.

(5) Sibiya, P. N.; Moloto, M. J. Synthesis, characterisation and antimicrobial effect of starch capped silver sulphide nanoparticles against *Escherichia coli* and *Staphylococcus aureus*. *Int. J. Nanotechnol.* **2017**, *14*, 385−398.

(6) Fakhri, A.; Pourmand, M.; Khakpour, R.; Behrouz, S. Structural, optical, photoluminescence and antibacterial properties of copper-doped silver sulfide nanoparticles. *J. Photochem. Photobiol., B* **2015**, *149*, 78−83.

(7) Delgado-Beleño, Y.; Martinez-Nuñez, C. E.; Cortez-Valadez, M.; Flores-Lopez, N. S.; Flores-Acosta, M. Optical properties of silver, silver sulfide and silver selenide nanoparticles and antibacterial applications. *Mater. Res. Bull.* **2018**, *99*, 385−392.

(8) Wang, J.; Sun, J. Y.; Huang, J.; Fakhri, A.; Gupta, V. K. Synthesis and its characterization of silver sulfide/nickel titanate/chitosan nanocomposites for photocatalysis and water splitting under visible light, and antibacterial studies. *Mater. Chem. Phys.* **2021**, *272*, No. 124990.

(9) Gupta, V. K.; Pathania, D.; Asif, M.; Sharma, G. Liquid phase synthesis of pectin-cadmium sulfide nanocomposite and its photocatalytic and antibacterial activity. *J. Mol. Liq.* **2014**, *196*, 107−112.

(10) Barman, J.; Sultana, F. Optoelectronic and antimicrobial activity of composite zinc oxide and cadmium sulphide quantum dots and application in water treatment. *Indian J. Pure Appl. Phys.* **2017**, *55*, 231−236.

(11) Shivashankarappa, A.; Sanjay, K. R. *Escherichia coli*- based synthesis of cadmium sulfide nanoparticles, characterization, antimicrobial and cytotoxicity studies. *Braz. J. Microbiol.* **2020**, *51*, 939−948.

(12) Jana, T. K.; Maji, S. K.; Pal, A.; Maiti, R. P.; Dolai, T. K.; Chatterjee, K. Photocatalytic and antibacterial activity of cadmium sulphide/zinc oxide nanocomposite with varied morphology. *J. Colloid Interface Sci.* **2016**, *480*, 9−16.

(13) Dorraji, M. S. S.; Ashjari, H. R.; Rasoulifard, M. H.; Rastgouy-Houjaghan, M. Polyurethane foam-cadmium sulfide nanocomposite with open cell structure: Dye removal and antibacterial applications. *Korean J. Chem. Eng.* **2017**, *34*, 547−554.

(14) Alsaggaf, M. S.; Elbaz, A. F.; El Badawy, S.; Moussa, S. H. Anticancer and Antibacterial Activity of Cadmium Sulfide Nanoparticles by Aspergillus niger. *Adv. Polym. Technol.* **2020**, *2020*, 1−13.

(15) Ashengroph, M.; Khaledi, A.; Bolbanabad, E. M. Extracellular biosynthesis of cadmium sulphide quantum dot using cell-free extract of Pseudomonas chlororaphis CHR05 and its antibacterial activity. *Process Biochem.* **2020**, *89*, 63−70.

(16) Liu, L.; Sun, M. Q.; Zhang, H. J.; Yu, Q. L.; Li, M. C.; Qi, Y.; Zhang, C. D.; Gao, G. D.; Yuan, Y. J.; Zhai, H. H.; Chen, W.; Alvarez, P. J. J. Facet Energy and Reactivity versus Cytotoxicity: The Surprising Behavior of CdS Nanorods. *Nano Lett.* **2016**, *16*, 688−694.

(17) Shalabayev, Z.; Baláž, M.; Khan, N.; Nurlan, Y.; Augustyniak, A.; Daneu, N.; Tatykaev, B. B.; Dutková, E.; Burashev, G.; Casas Luna, M.; Džunda, R.; Bureš, R.; Čelko, L.; Ilin, A.; Burkitbayev, M. Sustainable synthesis of cadmium sulfide applicable in photocatalysis, hydrogen production, and as an antibacterial agent using two mechanochemical protocols. *Nanomaterials* **2022**, *12*, No. 1250.

(18) Addae, E.; Dong, X. L.; McCoy, E.; Yang, C.; Chen, W.; Yang, L. J. Investigation of antimicrobial activity of photothermal therapeutic gold/copper sulfide core/shell nanoparticles to bacterial spores and cells. *J. Biol. Eng.* **2014**, *8*, No. 11.
(19) Wang, H. Y.; Hua, X. W.; Wu, F. G.; Li, B. L.; Liu, P. D.; Gu, N.; Wang, Z. F.; Chen, Z. Synthesis of Ultrastable Copper Sulfide Nanoclusters via Trapping the Reaction Intermediate: Potential Anticancer and Antibacterial Applications. *ACS Appl. Mater. Interfaces* **2015**, *7*, 7082−7092.
(20) Ahmed, K. B. A.; Anbazhagan, V. Synthesis of copper sulfide nanoparticles and evaluation of in vitro antibacterial activity and in vivo therapeutic effect in bacteria-infected zebrafish. *RSC Adv.* **2017**, *7*, 36644−36652.
(21) Ahmed, K. B. A.; Subramaniyan, S. B.; Banu, S. F.; Nithyanand, P.; Anbazhagan, V. Jacalin-copper sulfide nanoparticles complex enhance the antibacterial activity against drug resistant bacteria via cell surface glycan recognition. *Colloids Surf., B* **2018**, *163*, 209−217.
(22) Shalabayev, Z.; Baláž, M.; Daneu, N.; Dutková, E.; Bujňáková, Z.; Kaňuchová, M.; Danková, Z.; Balážová, L'.; Urakaev, F.; Tkáčiková, L.; Burkitbayev, M. Sulfur-Mediated Mechanochemical Synthesis of Spherical and Needle-Like Copper Sulfide Nanocrystals with Antibacterial Activity. *ACS Sustainable Chem. Eng.* **2019**, *7*, 12897−12909.
(23) Wang, Y.; Wang, W.; Liu, B. J.; Yu, D. Preparation of durable antibacterial and electrically conductive polyacrylonitrile fibers by copper sulfide coating. *J. Appl. Polym. Sci.* **2017**, *134*, No. 45496.
(24) Subramaniyan, S. B.; Vijayakumar, S.; Megarajan, S.; Kamlekar, R. K.; Anbazhagan, V. Remarkable Effect of Jacalin in Diminishing the Protein Corona Interference in the Antibacterial Activity of Pectin-Capped Copper Sulfide Nanoparticles. *ACS Omega* **2019**, *4*, 14049−14056.
(25) Gargioni, C.; Borzenkov, M.; D'Alfonso, L.; Sperandeo, P.; Polissi, A.; Cucca, L.; Dacarro, G.; Grisoli, P.; Pallavicini, P.; D'Agostino, A.; Taglietti, A. Self-Assembled Monolayers of Copper Sulfide Nanoparticles on Glass as Antibacterial Coatings. *Nanomaterials* **2020**, *10*, No. 352.
(26) Roy, S.; Rhim, J. W. Fabrication of Copper Sulfide Nanoparticles and Limonene Incorporated Pullulan/Carrageenan-Based Film with Improved Mechanical and Antibacterial Properties. *Polymers* **2020**, *12*, No. 2665.
(27) Bekhit, M.; El Naga, A. O. A.; El Saied, M.; Maksoud, M. I. A. A. Radiation-induced synthesis of copper sulfide nanotubes with improved catalytic and antibacterial activities. *Environ. Sci. Pollut. Res.* **2021**, *28*, 44467−44478.
(28) Liu, C.; Kong, D. S.; Hsu, P. C.; Yuan, H. T.; Lee, H. W.; Liu, Y. Y.; Wang, H. T.; Wang, S.; Yan, K.; Lin, D. C.; Maraccini, P. A.; Parker, K. M.; Boehm, A. B.; Cui, Y. Rapid water disinfection using vertically aligned MoS2 nanofilms and visible light. *Nat. Nanotechnol.* **2016**, *11*, 1098−1104.
(29) Yin, W. Y.; Yu, J.; Lv, F. T.; Yan, L.; Zheng, L. R.; Gu, Z. J.; Zhao, Y. L. Functionalized Nano-MoS2 with Peroxidase Catalytic and Near-Infrared Photothermal Activities for Safe and Synergetic Wound Antibacterial Applications. *ACS Nano* **2016**, *10*, 11000−11011.
(30) Yang, X.; Li, J.; Liang, T.; Ma, C. Y.; Zhang, Y. Y.; Chen, H. Z.; Hanagata, N.; Su, H. X.; Xu, M. S. Antibacterial activity of two-dimensional MoS2 sheets. *Nanoscale* **2014**, *6*, 10126−10133.
(31) Gao, Q.; Zhang, X.; Yin, W. Y.; Ma, D. Q.; Xie, C. J.; Zheng, L. R.; Dong, X. H.; Mei, L. Q.; Yu, J.; Wang, C. Z.; Gu, Z. J.; Zhao, Y. L. Functionalized MoS2 Nanovehicle with Near-Infrared Laser-Mediated Nitric Oxide Release and Photothermal Activities for Advanced Bacteria-Infected Wound Therapy. *Small* **2018**, *14*, No. 1802290.
(32) Cao, F. F.; Ju, E. G.; Zhang, Y.; Wang, Z. Z.; Liu, C. Q.; Li, W.; Huang, Y. Y.; Dong, K.; Ren, J. S.; Qu, X. G. An Efficient and Benign Antimicrobial Depot Based on Silver -Infused MoS2. *ACS Nano* **2017**, *11*, 4651−4659.
(33) Zhang, W. T.; Shi, S.; Wang, Y. R.; Yu, S. X.; Zhu, W. X.; Zhang, X.; Zhang, D. H.; Yang, B. W.; Wang, X.; Wang, J. L. Versatile molybdenum disulfide based antibacterial composites for in vitro enhanced sterilization and in vivo focal infection therapy. *Nanoscale* **2016**, *8*, 11642−11648.
(34) Mutalik, C.; Krisnawati, D. I.; Patil, S. B.; Khafid, M.; Atmojo, D. S.; Santoso, P.; Lu, S. C.; Wang, D. Y.; Kuo, S. R. Phase-Dependent MoS2 Nanoflowers for Light-Driven Antibacterial Application. *ACS Sustainable Chem. Eng.* **2021**, *9*, 7904−7912.
(35) Xu, J. G.; Cai, R.; Zhang, Y. G.; Mu, X. Y. Molybdenum disulfide-based materials with enzyme-like characteristics for biological applications. *Colloids Surf., B* **2021**, *200*, No. 111575.
(36) Zhao, Y. C.; Jia, Y. X.; Xu, J. Y.; Han, L.; He, F.; Jiang, X. Y. The antibacterial activities of MoS2 nanosheets towards multi-drug resistant bacteria. *Chem. Commun.* **2021**, *57*, 2998−3001.
(37) Kumar, P.; Roy, S.; Sarkar, A.; Jaiswal, A. Reusable MoS2-Modified Antibacterial Fabrics with Photothermal Disinfection Properties for Repurposing of Personal Protective Masks. *ACS Appl. Mater. Interfaces* **2021**, *13*, 12912−12927.
(38) Shi, J. P.; Li, J.; Wang, Y.; Cheng, J. J.; Zhang, C. Y. Recent advances in MoS2-based photothermal therapy for cancer and infectious disease treatment. *J. Mater. Chem. B* **2020**, *8*, 5793−5807.
(39) Mani, S. K.; Manickam, S.; Muthusamy, V.; Thangaraj, R. Antimicrobial Activity and Photocatalytic Degradation Properties of Zinc Sulfide Nanoparticles Synthesized by Using Plant Extracts. *J. Nanostruct.* **2018**, *8*, 107−118.
(40) Sathishkumar, M.; Rajamanickam, A. T.; Saroja, M. Characterization, antimicrobial activity and photocatalytic degradation properties of pure and biosynthesized zinc sulfide nanoparticles using plant extracts. *J. Mater. Sci.: Mater. Electron.* **2018**, *29*, 14200−14209.
(41) Kannan, S.; Subiramaniyam, N. P.; Sathishkumar, M. A novel green synthesis approach for improved photocatalytic activity and antibacterial properties of zinc sulfide nanoparticles using plant extract of Acalypha indica and Tridax procumbens. *J. Mater. Sci.: Mater. Electron.* **2020**, *31*, 9846−9859.
(42) Morshedtalab, Z.; Rahimi, G.; Emami-Nejad, A.; Farasat, A.; Mohammadbeygi, A.; Ghaedamini, N.; Negahdary, M. Antibacterial Assessment of Zinc Sulfide Nanoparticles against *Streptococcus pyogenes* and *Aeinetobacter baumannii*. *Curr. Top. Med. Chem.* **2020**, *20*, 1042−1055.
(43) Giridhar, M.; Naik, H. S. B.; Prabhakar, M. C.; Naik, M. M.; Ballesh, N.; Mahesh, M. C. Synthesis, characterization and antibacterial activity of water-soluble dye-capped zinc sulphide nanoparticles from waste Zn-C battery. *Bull. Mater. Sci.* **2021**, *44*, No. 6.
(44) Li, G. P.; Zhai, J. F.; Li, D.; Fang, X. N.; Jiang, H.; Dong, Q. Z.; Wang, E. K. One-pot synthesis of monodispersed ZnS nanospheres with high antibacterial activity. *J. Mater. Chem.* **2010**, *20*, 9215−9219.
(45) Fakhri, A.; Behrouz, S.; Pourmand, M. Synthesis, photocatalytic and antimicrobial properties of SnO2, SnS2 and SnO2/SnS2 nanostructure. *J. Photochem. Photobiol., B* **2015**, *149*, 45−50.
(46) He, X. Y.; Gan, J. G.; Fakhri, A.; Dizaji, B. F.; Azarbaijan, M. H.; Hosseini, M. Preparation of ceric oxide and cobalt sulfide-ceric oxide/cellulose-chitosan nanocomposites as a novel catalyst for efficient photocatalysis and antimicrobial study. *Int. J. Biol. Macromol.* **2020**, *143*, 952−957.
(47) Ashraf, M. A.; Li, C.; Zhang, D. Q.; Fakhri, A. Graphene oxides as support for the synthesis of nickel sulfide-indium oxide nanocomposites for photocatalytic, antibacterial and antioxidant performances. *Appl. Organomet. Chem.* **2020**, *34*, No. e5354.
(48) Tiss, B.; Moualhi, Y.; Bouguila, N.; Kraini, M.; Alaya, S.; Croitoru, C.; Ghiuta, I.; Cristea, D.; Patroi, D.; Moura, C.; Cunha, L. Influence of the Physical Properties on the Antibacterial and Photocatalytic Behavior of Ag-Doped Indium Sulfide Film Deposited by Spray Pyrolysis. *Coatings* **2021**, *11*, No. 370.
(49) Lokhande, A. C.; Shelke, A.; Babar, P. T.; Kim, J.; Lee, D. J.; Kim, I. C.; Lokhandee, C. D.; Kim, J. H. Novel antibacterial application of photovoltaic Cu_2SnS_3 (CTS) nanoparticles. *RSC Adv.* **2017**, *7*, 33737−33744.
(50) Kumar, R. S.; Maddirevula, S.; Easwaran, M.; Dananjaya, S. H. S.; Kim, M. D. Antibacterial activity of novel Cu2ZnSnS4 nano-

https://doi.org/10.1021/acsomega.2c01657
ACS Omega 2022, 7, 27164−27171

particles against pathogenic strains. *RSC Adv.* **2015**, *5*, 106400−106405.
(51) Ocakoglu, K.; Dizge, N.; Colak, S. G.; Ozay, Y.; Bilici, Z.; Yalcin, M. S.; Ozdemir, S.; Yatmaz, H. C. Polyethersulfone membranes modified with CZTS nanoparticles for protein and dye separation: Improvement of antifouling and self-cleaning performance. *Colloids Surf., A* **2021**, *616*, No. 126230.
(52) Song, C. Q.; Li, T. C.; Guo, W.; Gao, Y.; Yang, C. Y.; Zhang, Q.; An, D.; Huang, W. C.; Yan, M.; Guo, C. S. Hydrophobic Cu12Sb4S13-deposited photothermal film for interfacial water evaporation and thermal antibacterial activity. *New J. Chem.* **2018**, *42*, 3175−3179.
(53) Kulkarni, P.; Nataraj, S. K.; Balakrishna, R. G.; Nagaraju, D. H.; Reddy, M. V. Nanostructured binary and ternary metal sulfides: synthesis methods and their application in energy conversion and storage devices. *J. Mater. Chem. A* **2017**, *5*, 22040−22094.
(54) Liu, Y. C.; Li, Y.; Kang, H. Y.; Jin, T.; Jiao, L. F. Design, synthesis, and energy-related applications of metal sulfides. *Mater. Horiz.* **2016**, *3*, 402−421.
(55) Baláž, P.; Achimovičová, M.; Baláž, M.; Billik, P.; Cherkezova-Zheleva, Z.; Criado, J. M.; Delogu, F.; Dutková, E.; Gaffet, E.; Gotor, F. J.; Kumar, R.; Mitov, I.; Rojac, T.; Senna, M.; Streletskii, A.; Wieczorek-Ciurowa, K. Hallmarks of mechanochemistry: from nanoparticles to technology. *Chem. Soc. Rev.* **2013**, *42*, 7571−7637.
(56) Baláž, P.; Baláž, M.; Achimovičová, M.; Bujňáková, Z.; Dutková, E. Chalcogenide mechanochemistry in materials science: insight into synthesis and applications (a review). *J. Mater. Sci.* **2017**, *52*, 11851−11890.
(57) Gock, E.; Kurrer, K. E. Eccentric vibratory mills-a new energy efficient way for pulverization. *Erzmetall* **1996**, *49*, 434−442.
(58) Baláž, P.; Hegedüs, M.; Reece, M.; Zhang, R.; Su, T.; Škorvánek, I.; Briančin, J.; Baláž, M.; Mihálik, M.; Tešinský, M.; Achimovičová, M. Mechanochemistry for thermoelectrics: Nanobulk $Cu_6Fe_2SnS_8/Cu_2FeSnS_4$ composite synthesized in an industrial mill. *J. Electron. Mater.* **2019**, *48*, 1846−1856.
(59) Baláž, M.; Dobrozhan, O.; Tešinský, M.; Zhang, R.-Z.; Džunda, R.; Dutková, E.; Rajňák, M.; Chen, K.; Reece, M. J.; Baláž, P. Scalable and environmentally friendly mechanochemical synthesis of nanocrystalline rhodostannite (Cu2FeSn3S8). *Powder Technol.* **2021**, *388*, 192−200.
(60) Baláž, P.; Hegedüs, M.; Baláž, M.; Daneu, N.; Šiffalovič, P.; Bujňáková, Z.; Tóthová, E.; Tešinský, M.; Achimovičová, M.; Briančin, J.; Dutková, E.; Kaňuchová, M.; Fabián, M.; Kitazono, S.; Dobrozhan, O. Photovoltaic Materials: Cu2ZnSnS4 (CZTS) Nanocrystals Synthesized via Industrially Scalable, Green, One-step Mechanochemical Process. *Prog. Photovoltaics* **2019**, *27*, 798−811.
(61) Baláž, P.; Guilmeau, E.; Daneu, N.; Dobrozhan, O.; Baláž, M.; Hegedus, M.; Barbier, T.; Achimovičová, M.; Kaňuchová, M.; Briančin, J. Tetrahedrites synthesized via scalable mechanochemical process and spark plasma sintering. *J. Eur. Ceram. Soc.* **2020**, *40*, 1922−1930.
(62) Hegedüs, M.; Achimovičová, M.; Hui, H. J.; Guelou, G.; Lemoine, P.; Fourati, I.; Juraszek, J.; Malaman, B.; Baláž, P.; Guilmeau, E. Promoted crystallisation and cationic ordering in thermoelectric Cu26V2Sn6S32 colusite by eccentric vibratory ball milling. *Dalton Trans.* **2020**, *49*, 15828−15836.
(63) Baláž, P.; Achimovičová, M.; Baláž, M.; Chen, K.; Dobrozhan, O.; Guilmeau, E.; Hejtmánek, J.; Knížek, K.; Kubíčková, L.; Levinský, P.; Puchý, V.; Reece, M. J.; Varga, P.; Zhang, R.-Z. Thermoelectric CuS-Based Materials Synthesized via a Scalable Mechanochemical Process. *ACS Sustainable Chem. Eng.* **2021**, *9*, 2003−2016.
(64) Dutková, E.; Sayagués, M. J.; Fabián, M.; Baláž, M.; Achimovičová, M. Mechanochemically synthesized ternary chalcogenide Cu3SbS4 powders in a laboratory and an industrial mill. *Mater. Lett.* **2021**, *291*, No. 129566.
(65) Baláž, P.; Hegedüs, M.; Achimovičová, M.; Baláž, M.; Tešinský, M.; Dutková, E.; Kaňuchová, M.; Briančin, J. Semi-industrial green mechanochemical syntheses of solar cell absorbers based on quaternary sulfides. *ACS Sustainable Chem. Eng.* **2018**, *6*, 2132−2141.
(66) Achimovičová, M.; Baláž, M.; Girman, V.; Kurimský, J.; Briančin, J.; Dutková, E.; Gaborová, K. Comparative Study of Nanostructured CuSe Semiconductor Synthesized in a Planetary and Vibratory Mill. *Nanomaterials* **2020**, *10*, No. 2038.
(67) Metchnikoff, E. *The Founders of Modern Medicine: Pasteur, Koch, Lister*; Walden Publications, 1939; p 387.
(68) Rojas, J. J.; Ochoa, V. J.; Ocampo, S. A.; Muñoz, J. F. Screening for antimicrobial activity of ten medicinal plants used in Colombian folkloric medicine: A possible alternative in the treatment of non-nosocomial infections. *BMC Complementary Altern. Med.* **2006**, *6*, No. 2.
(69) Tsuzuki, T.; McCormick, P. G. Mechanochemical synthesis of nanoparticles. *J. Mater. Sci.* **2004**, *39*, 5143−5146.
(70) Boldyrev, V. V.; Tkacova, K. Mechanochemistry of solids: Past, present, and prospects. *J. Mater. Synth. Process.* **2000**, *8*, 121−132.
(71) Baláž, M. *Environmental Mechanochemistry: Recycling Waste into Materials Using High-Energy Ball Milling*; Springer, 2021; p 619.
(72) Li, J. J.; Shen, J.; Li, Z. Q.; Li, X. D.; Sun, Z.; Hu, Z. G.; Huang, S. M. Wet chemical route to the synthesis of kesterite Cu2ZnSnS4 nanocrystals and their applications in lithium ion batteries. *Mater. Lett.* **2013**, *92*, 330−333.
(73) Salton, M. R. J.; Kim, K. S.; Baron, S. Structure. In *Medical Microbiology*, 4th ed.; University of Texas Medical Branch: Galveston (TX), 1996.
(74) Valodkar, M.; Modi, S.; Pal, A.; Thakore, S. Synthesis and anti-bacterial activity of Cu, Ag and Cu-Ag alloy nanoparticles: A green approach. *Mater. Res. Bull.* **2011**, *46*, 384−389.
(75) Hou, X.; Li, Y.; Yan, J. J.; Wang, C. W. Highly efficient photocatalysis of p-type Cu2ZnSnS4 under visible-light illumination. *Mater. Res. Bull.* **2014**, *60*, 628−633.
(76) Chirayil, C. J.; Abraham, J.; Mishra, R. K.; George, S. C.; Thomas, S. Instrumental Techniques for the Characterization of Nanoparticles. In *Thermal and Rheological Measurement Techniques for Nanomaterials Characterization*; Elsevier, 2017; Vol. 3, pp 1−36.
(77) Dutková, E.; Bujňáková, Z.; Kováč, J.; Škorvánek, I.; Sayagues, M. J.; Zorkovská, A.; Kováč, J., Jr.; Baláž, P. Mechanochemical synthesis, structural, magnetic, optical and electrooptical properties of CuFeS2 nanoparticles. *Adv. Powder Technol.* **2018**, *29*, 1820−1826.
(78) Dutková, E.; Sayagués, M. J.; Fabián, M.; Kováč, J.; Baláž, M.; Stahorský, M. Mechanochemical synthesis of ternary chalcogenide chalcostibite CuSbS2 and its characterization. *J. Mater. Sci.: Mater. Electron.* **2021**, *32*, 22898−22909.
(79) Mitchell, T. K.; Nguyen, A. V.; Evans, G. M. Heterocoagulation of chalcopyrite and pyrite minerals in flotation separation. *Adv. Colloid Interface Sci.* **2005**, *114*−*115*, 227−237.
(80) Wang, X.; Forssberg, E.; Bolin, N. J. The aqueous and surface chemistry of activation in the flotation of sulphide minerals—A review. Part II: A surface precipitation model. *Miner. Process. Extr. Metall. Rev.* **1989**, *4*, 167−199.

https://doi.org/10.1021/acsomega.2c01657
ACS Omega 2022, 7, 27164−27171